




 Cite this: *RSC Adv.*, 2022, 12, 7898

# Multi-responsive and conductive bilayer hydrogel and its application in flexible devices†

 Dongyang Yu,  Yanhua Teng,\* He Feng, Xiuling Lin, Jianjun Li, Qingping Wang and Changguo Xue \*

Multi-stimuli-responsive hydrogels are intelligent materials that present advantages for application in soft devices compared with conventional machines. In this paper, we prepared a bilayer hydrogel consisting of a poly(2-(dimethylamino)ethyl methacrylate) layer and a poly(*N*-isopropylacrylamide) layer. The hydrogel responded to temperature, pH, NaCl, and ethanol by undergoing bending deformation. At 40 °C, it only took 23 s for the hydrogel to bend nearly 300°. Carbon black was also introduced into the hydrogel network to render it conductive. Based on its multi-stimuli-responsive properties and conductivity, the hydrogel was used to construct a 4-arm gripper, thermistor, and finger movement monitor. The time required to grip and release an object was 141 s. The resistance changed with temperature, which affected the brightness of an LED. Finger motions were monitored, and the bending angle could be distinguished.

 Received 21st December 2021  
 Accepted 6th March 2022

DOI: 10.1039/d1ra09232d

[rsc.li/rsc-advances](https://rsc.li/rsc-advances)

## 1. Introduction

Hydrogels are three-dimensional networks of soft materials composed of polymers and water molecules that present the properties of both solids and fluids.<sup>1–3</sup> By absorbing or exuding water molecules, hydrogels can swell or de-swell, resulting in deformation. In recent years, smart hydrogels have become a research hotspot due to their stimuli-responsive properties.<sup>4–6</sup> After adding functional molecules or monomers, smart hydrogels become responsive to one or more stimuli such as temperature, pH, light, magnetic fields, *etc.*<sup>7–11</sup> resulting in various deformation modes, *e.g.*, shrinkage/expansion,<sup>12–14</sup> bending,<sup>15–17</sup> twisting,<sup>18,19</sup> or composite behaviors.<sup>20–22</sup>

In recent decades, bilayer hydrogels have garnered considerable attention from researchers because they can undergo multiple deformation modes. The different components of the two layers result in independent responses to various stimuli. Inspired by Mimosa, Zheng *et al.*<sup>23</sup> prepared a bilayer hydrogel *via* a moulding method that achieved multi-stimuli-responsiveness because it contained poly(acrylic acid) and poly(*N*-isopropylacrylamide). A soft gripper was fabricated by simply connecting a hydrogel flower to cotton fiber. Xiao *et al.*<sup>24</sup> synthesized a bilayer hydrogel consisting of poly([2-(methacryloyloxy)ethyl]trimethylammonium chloride) and poly[*N*-(2-hydroxyethyl)acrylamide], which was responsive to different salt types and salt concentrations. Furthermore, an eight-arm

gripper made of a bilayer hydrogel could grasp and release an object. Wang *et al.*<sup>25</sup> prepared a strong-interfacial bilayer hydrogel consisting of a shape-memory layer and an elastic layer. The bilayer hydrogel underwent different deformations *via* various heating-stretching modes. Most double-layer hydrogels have multi-stimuli-responsive properties and can be used for grasping functions.<sup>23,24,26,27</sup>

To develop additional applications, conductivity is required. Similar to single-layer hydrogels, methods to improve the conductivity of bilayer hydrogels include introducing conductive materials into hydrogels. Navaei *et al.*<sup>28</sup> prepared conductive gelatin-based hydrogels where gold nanorods promoted electrical conductivity and enhanced the mechanical stiffness. Xia and co-workers<sup>29</sup> fabricated a hydrogel-based wearable strain sensor consisting of polyacrylamide (PAM) and chitosan (CS). The conductivity of the hydrogel was improved by increasing the amount of carboxyl-functionalized multi-walled carbon nanotubes (MWCNTs), which ionically cross-linked with CS. In the work of Chen *et al.*,<sup>30</sup> a multifunctional conductive hydrogel was prepared in which polyaniline (PANI) provided electronic conductivity, and Fe<sup>3+</sup> and poly(4-styrenesulfonate) (PSS) provided ionic conductivity. Ying *et al.*<sup>31</sup> designed and synthesized an AIskin with ionic conductivity, presenting high stretchability and sensitivity. In addition to strain sensors, a promising application as soft diode was initially prepared and functioned.

In this paper, a bilayer hydrogel consisting of poly(*N*-isopropylacrylamide) (PNIPAM) and poly(2-(dimethylamino)ethyl methacrylate) (PDMAEMA) layers was prepared. The bilayer hydrogel was rendered multi-stimuli-responsive by adding PNIPAM and PDMAEMA as functional monomers.<sup>32–35</sup> The

School of Materials Science and Engineering, Anhui University of Science and Technology, China. E-mail: tyhqqr@126.com; chgxue@foxmail.com

† Electronic supplementary information (ESI) available. See DOI: 10.1039/d1ra09232d



bilayer hydrogel was tested for its response to multiple stimuli, including temperature, pH, salt, and ethanol. These stimuli caused the composite to bend due to the deformation of the two individual layers. In addition, the responsive behaviors of the bilayer hydrogel and each single-layer hydrogel and their response mechanisms to multiple stimuli are described. Further, the conductivity of the bilayer hydrogel was improved. In the PDMAEMA layer (D layer), the addition of PSS, a polyelectrolyte, provided ionic conductivity and electrostatic interactions that enhanced the stiffness. While in the PNIPAM layer, carbon black was added, which offered electronic conductivity. Compared to the works mentioned above, for multiple stimuli-responsive properties and conductivity, two individual properties of hydrogels, 4-arm gripper and strain sensor as conventional applications were fabricated. Additionally, this paper attempted to prepare an organic thermistor, which was a combination of stimuli-responsiveness and conductivity.

## 2. Experimental section

### 2.1 Materials

Carbon black (CB, 99.9%) was purchased from Alfa Aesar. Sodium dodecyl sulfonate (SDS, 92.5–100.5%), *N,N,N',N'*-tetramethylethylenediamine (TEMED, 99%), 2-(dimethylamino) ethyl methacrylate (DMAEMA, 99%), poly(ethylene glycol)diacrylate (PEGDA, average  $M_w \sim 575$  Da) and poly(sodium-p-styrene sulfonate) (PSS, average  $M_w \sim 70\,000$  Da, powder) were purchased from Macklin (Shanghai, China). Ammonium persulfate (APS, 98%) was purchased from Sinopharm Chemical Reagent Co., Ltd. Poly(vinyl alcohol) (PVA-124) and *N*-isopropylacrylamide (NIPAM, 98%) were purchased from Aladdin (Shanghai, China). SYLGARDTM 184 Silicone Elastomer Kit (PDMS) was purchased from Dow Corning Co., Ltd. All reagents were used without further purification.

### 2.2 Preparation of bilayer hydrogels

**2.2.1 Preparation of PVA/CB dispersion.** 30 mg SDS and 60 mg CB were added in 20 mL deionized water. Then the mixture was stirred for 1 h and then ultrasonicated for 2 h, obtaining CB dispersion. By adding 2.0 g PVA and stirring at 90 °C for 2 h, the CB/PVA dispersion was acquired.

**2.2.2 Preparation of pre-polymerization solution.** Under stirring, 1.0 g DMAEMA, 120  $\mu\text{L}$  PEGDA and 0.1 g PSS were added in 4.0 g  $\text{H}_2\text{O}$  to acquire the pre-polymerization solution of the D layer. Similarly, 1.0 g NIPAM, 45  $\mu\text{L}$  PEGDA, 400  $\mu\text{L}$  TEMED solution (100 mg  $\text{mL}^{-1}$ ) and 2.0 g PVA/CB dispersion were added in 2.0 g  $\text{H}_2\text{O}$  to acquire the pre-polymerization solution of the N layer.

**2.2.3 Preparation of the bilayer hydrogel.** After adding 400  $\mu\text{L}$  APS solution (100 mg  $\text{mL}^{-1}$ ), the pre-polymerization solution of the D layer was poured into the silica mould coated with cross-linked PDMS and polymerized for 5 min at 25 °C as the first layer. Subsequently, the pre-polymerization solution of the N layer mixed with 400  $\mu\text{L}$  APS solution (100 mg  $\text{mL}^{-1}$ ) was poured onto the first layer. Then, the mould was sealed for 24 h. After polymerization, the bilayer hydrogel was prepared.

### 2.3 Preparation of 4-arm grippers

The 4-arm gripper was assembled by placing two strips of the bilayer hydrogel crosswise and then piercing them by a thumb-tack with the D layer facing upside. The object for gripping was a copper sheet with a weight of 1.15 g.

### 2.4 Preparation of finger movement monitor

The bilayer hydrogel was cut into a strip with a size of 1 cm  $\times$  4 cm. Then, the hydrogel was tightly attached to a finger joint. Both ends of the hydrogel were affixed with a copper net and then tied to the finger with insulating tape. The wires connected the copper net and multi-meter through crocodile clips.

### 2.5 Characterization

The morphology of the hydrogels was characterized by immersing the prepared hydrogel in deionized water for 24 h to remove unreacted substances and then freeze-drying it for 24 h. The freeze-dried hydrogel was cut into slices and then sputtered with gold. Then, the morphology of the hydrogels was recorded by scanning electron microscopy (SEM) with an operating voltage of 5 kV.

### 2.6 Stimuli-responsiveness of the hydrogel

In this article, the environmental stimuli were temperature, pH, salt, and absolute ethanol. It should be noted that the pH values were 0 and 14, represented by 1 M hydrochloric acid (HCl) and 1 M NaOH solution. NaCl was used as the salt because its cation and anion carry only one charge each, just like HCl and NaOH. NaCl is a strong electrolyte and can be regarded as a neutral environment (pH = 7) to maintain the same ion concentration. In addition, NaCl solutions with different concentration (1 M, 2 M, 3 M, 4 M and 5 M) were used to further explore salt-responsive property. The bilayer hydrogels were cut into strips and immersed in different liquid environments. For a more convenient calculation, the bent hydrogels were regarded as the arc of a circle, which would be detailedly discussed in the following chapter; therefore, the center angle could be easily obtained on the figure, and the curvature is the reciprocal of the radius. The actual values of center angle and curvature of the circle were calculated by selecting the reference object. The center angle and curvature of the arc were both used to describe the bending behavior of the hydrogel.

### 2.7 Conductivity

Electrical resistance was selected to represent the conductivity of the bilayer hydrogel. The electrical resistance was measured with a multi-meter (Pro'skit MT-1820).

## 3. Results and discussion

### 3.1 Preparation of hydrogels

In this work, PDMAEMA/PNIPAM bilayer hydrogels were designed and prepared *via* the casting method. As shown in Fig. 1, the first step was to prepare the D layer, and when the polymerization degree of the D layer approached the gel point



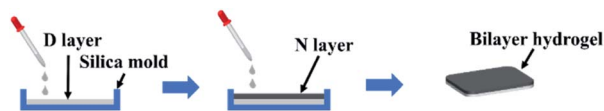


Fig. 1 Schematic illustration of bilayer hydrogel preparation.

(the viscosity of the D layer increased, and the hydrogel presented solid properties), the mixture of the N layer was added. Then, the mould was sealed for 12 h. In the D layer, since sulfonyl and amino groups carry opposite charges, electrostatic interactions were formed between PDMAEMA and PSS, forming a semi-crosslinked network. In the N layer, the addition of PVA improved the strength and toughness by forming hydrogen bonds between acrylamides in PNIPAM and hydroxyls in PVA. TEMED was used to promote the homolysis of APS, reducing the initiation temperature. CB was added to further enhance the mechanical strength and provide electrically-conductive properties, along with SDS as the dispersant and stabilizer.

SEM images provided detailed information about the D layer, N layer, and their interface. As shown in Fig. 2a and b, the D layer and the N layer possessed different morphologies. In Fig. 2c, the interface between the two layers was clear. Fig. 2d additionally presented the differences in color.

### 3.2 Deformation mechanism and stimuli-responsive behavior of bilayer hydrogels

The bending deformation of bilayer hydrogels depends on the swelling ratio of the two layers, which respectively present their unique properties; however, the bending of the bilayer hydrogel depends on the combined effect of the two layers. Therefore,

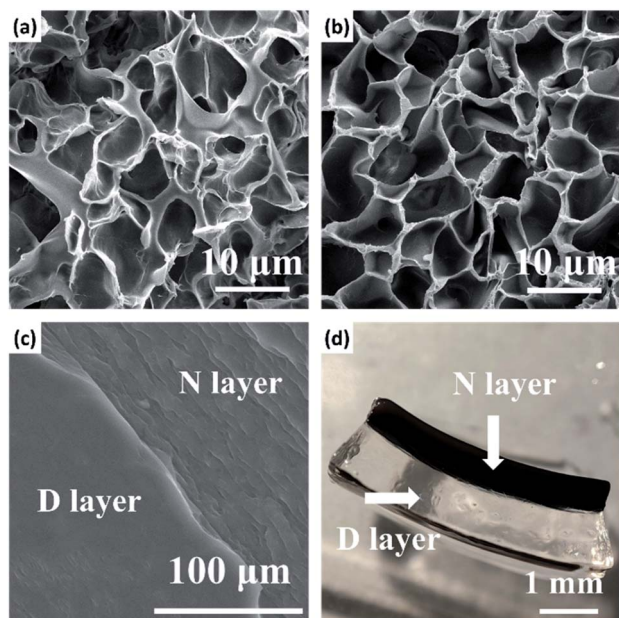


Fig. 2 SEM images of (a) D layer, (b) N layer and (c) the interface; (d) photo of the prepared bilayer hydrogel cut in a size of 4.2 mm × 2.2 mm × 1.3 mm.

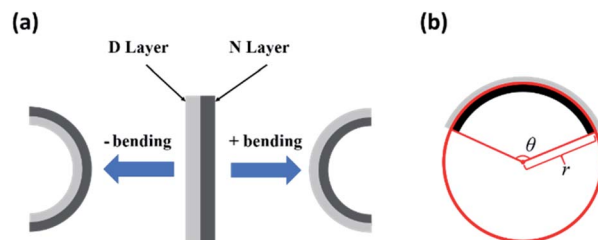


Fig. 3 (a) Positive and negative bending directions; (b) simplified model for calculating the center angle and curvature of the bent hydrogel ( $\theta$  is the center angle corresponding to the arc, and  $r$  is the radius of the circle).

multi-stimuli tests were conducted, resulting in two bending directions. In Fig. 3a, the positive (+) bending and negative (−) bending were artificially specified. When bending, the shape of the hydrogel was treated as the arc of a circle, as shown in Fig. 3b, which simplifies the data processing but slightly decreases the data accuracy. Additionally, the corresponding single-layer hydrogels were synthesized and tested, which provided supplementary data, as shown in Fig. S1.† The thickness of each single-layer hydrogel was less than 1 mm; therefore, the area change was calculated by  $S/S_0$ , where  $S_0$  is the original area, and  $S$  is the area after the application of a stimulus or stimuli.

In the thermal-responsive test, the bilayer hydrogel bent positively when immersed in water at 40 °C. As Fig. 4a shows, it only took 23 s for the bilayer hydrogel to bend to nearly 300°, and the curvature increased from 0.29 to 1.36. Both PNIPAM and PDMAEMA are thermal-responsive polymers with different lower critical solution temperatures (LCSTs). When the temperature exceeds the LCST, the hydrophobic interactions between polymer chains strengthen, and the hydrogen bonds weaken, resulting in the rapid collapse of polymer chains. Macroscopically, this causes the hydrogel to shrink. The LCST of PNIPAM and PDMAEMA were around 32 °C and 40 °C, respectively; thus, the de-swelling degree of the N layer was greater than that of the D layer at the same temperature, which was confirmed by Fig. S1;† however, the recovery time was much longer, as shown in Fig. 4b. It took 1800 s to recover at room temperature, which can be explained intuitively as a rapid squeeze but slow re-absorption.<sup>36</sup> By comparing the shape of the hydrogel before and after heating, the hydrogel both bent and shrank, as shown in Fig. 4 and S1.† It should be pointed out that

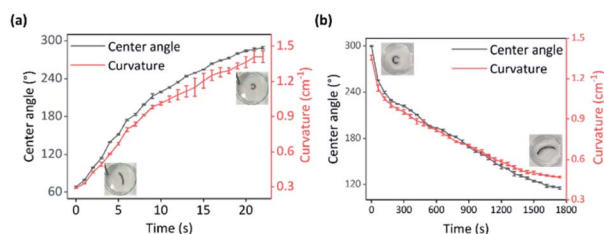


Fig. 4 Center angles and curvatures of the bilayer hydrogel at 40 °C (a) and its recovery (b).





when the gel was formed, the polymer did not dissolve; thus, the LCST could not be satisfied by definition. Because the polymer chains still shrank or relaxed, the volume phase transition temperature (VPTT) was used to represent the thermo-sensitive properties of the hydrogel.

Two factors, the temperature and amount of SDS in the CB dispersion (the original concentration of SDS was  $0.75 \text{ mg mL}^{-1}$ ), were investigated for their influence on the thermal-sensitive properties of hydrogels. A series of temperature gradients was set, as shown in Fig. S2.† To display the data more intuitively, the average rates of the center angle ( $R_a$ ) and curvature ( $R_b$ ) were used.

$$R_a = \frac{\theta_e - \theta_0}{t} \quad (1)$$

where  $\theta_e$  is the final value of the center angle,  $\theta_0$  is the initial value of the center angle, and  $t$  is the total time.

$$R_b = \frac{C_e - C_0}{t} \quad (2)$$

where  $C_e$  is the final curvature,  $C_0$  is the initial curvature, and  $t$  is the total time.

It is shown in Fig. 5a that as the temperature rose, the average rate of both parameters increased, presenting a positive correlation. A higher temperature led to a more rapid increase in the entropy of water molecules, which resulted in faster breaking of hydrogen bonds between the amide groups and water molecules, which facilitated hydrophobic interactions among isopropyl groups. In terms of recoverability, excessive stimulus caused irreversible damage to the hydrogels.

Increasing the SDS concentration to  $1.5 \text{ mg mL}^{-1}$  extremely prolonged the response time. In Fig. 5b, the change in the center angle and curvature maintained the same trend as the experiment above at  $40^\circ\text{C}$ , but the response time increased nearly ten times, and the bending degree decreased compared to the original value. As for the recovery (Fig. S3†), the time was much shorter than in the original concentration. One reason for this was that a large number of SDS molecules blocked the hydrophobic interactions between isopropyl groups with alkanes at the end of SDS, which increased the VPTT.<sup>37</sup> Another reason was that SDS created repulsive electrostatic interactions that inhibited the collapse of PNIPAM chains.<sup>38</sup> These two factors did not change the bending direction, but they did affect the rate.

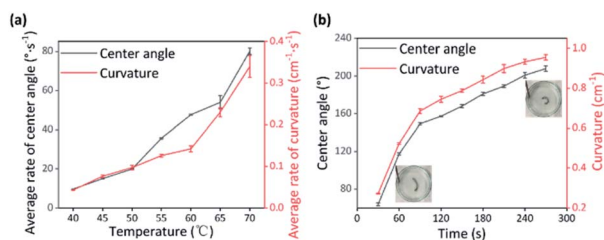


Fig. 5 (a) Average rate of the two parameters; (b) center angles and curvature change of bilayer hydrogel in solution with a higher concentration of SDS ( $1.5 \text{ mg mL}^{-1}$ ).

In the pH-responsive test, 1 M hydrochloric acid (HCl) and 1 M NaOH solution were used to represent acidic and alkaline environments, respectively. In contrast, 1 M NaCl solution is used as a neutral environment, while maintaining the same ion concentration. When placed in acidic, alkaline, and neutral environments with the same ion concentration, the bilayer hydrogel bent towards the positive direction, but at different rates. In an acidic environment, the bilayer hydrogel bent positively. The center angle rose to  $182^\circ$ , and the curvature rose to 0.79 over 570 s, as shown in Fig. 6a. In an alkaline environment (Fig. 6c), it took 200 s for the center angle to reach  $300^\circ$  and for the curvature to rise to 1.09, which shows a shorter response time and higher bending degree, while the bending direction was unchanged. In a neutral environment, the hydrogel also bent positively. In Fig. 6e, the center angle and curvature increased more slowly than the former two, with values of  $187^\circ$  and 0.86, respectively.

The two layers had different response mechanisms. In the D layer, the equilibrium swelling behavior was related to the degree of ion dissociation. The pH of the solution directly affected the degree of ion dissociation of the electrolyte. In the PDMAEMA chains *N,N*-dimethylaminoethyl, generally became more hydrophilic after the protonation of its many amino groups. At the same time, electrostatic repulsion between the same ions led to the diffusion of polymer chains, causing swelling. Under alkaline conditions, the polymer chains agglomerated due to the deprotonation of the tertiary amino groups and hydrophobic interactions, resulting in the deswelling of the hydrogel. In the N layer, the PNIPAM chains were ion-responsive. Lee *et al.* showed that some salts decrease the LCST of thermal-responsive polymers (the “salting-in

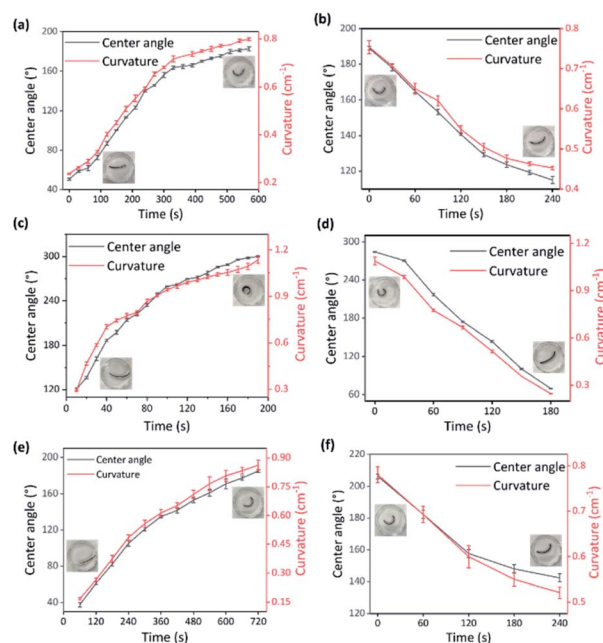


Fig. 6 The center angles and curvatures of bilayer hydrogel in solutions of 1 M HCl (a), 1 M NaOH (c), 1 M NaCl (e) and their respective recovery (b), (d), (f).



effect”), and others increase the LCST (the “salting-out effect”), which is true for NaCl.<sup>39</sup> On the one hand, the addition of NaCl increased the hydrogen bonds between water molecules, therefore decreasing those between water and hydrophilic chains. On the other hand, it increased the polarity of water molecules, enhancing the hydrophobic interactions between polymer chains. These combined factors caused the PNIPAM hydrogel to shrink in environments with a high ion concentration (Fig. S1b†).

It can be judged from the curves in Fig. 6a, c, and e that the response rate slowed down over time. We speculate that upon increasing the concentration of ions in the hydrogel, the osmotic pressure difference between the inside and outside of the hydrogel decreased gradually, which blocked the penetration of additional ions. There were also fewer unreacted responsive groups over time. During recovery procedure, whether in an acidic, alkaline, or neutral environment, the time was shorter than the response time, as shown in Fig. 6b, d, and f. We speculated that water molecules can engage in electrostatic interactions with ions.

Additionally, the bilayer hydrogel was immersed in NaCl solution with different concentration (1 M, 2 M, 3 M, 4 M and 5 M) to further explore the salt-responsive property. The change in center angle and curvature of the bilayer hydrogel are shown in Fig. S4(a) and (b).† To display the data more intuitively, the average rates of the center angle and curvature were used as Fig. S4(c)† shows. It turned out that the average rate of the two parameters was positively correlated with the concentration of NaCl solution.

Apart from temperature, pH, and ion concentration, the bilayer hydrogel also responded to ethanol. Different from the previous test results, when the hydrogel was immersed in ethanol, it bent towards the negative direction. In Fig. 7a, it took 1140 s for the center angle and curvature to increase to 150° and 0.58. The mechanism in the N layer was that ethanol was a better solvent for NIPAM; thus, the hydrogel swelled, as shown in Fig. S1b.† In the D layer, the mechanism is still unknown. We deduced that ethanol affects hydrogen bonds between water molecules and hydrophilic groups, which reduced the LCST. In Fig. 7b, the recovery time was approximately one-fifth that of the response time. We suspect that the attraction of a large number of water molecules to ethanol molecules was greater than to the hydrogel.

In temperature, pH, and salt tests, the hydrogel bent positively, while in ethanol, it bent negatively. Among the stimuli-

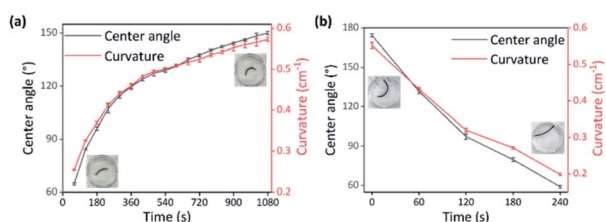


Fig. 7 Center angles and curvatures of bilayer hydrogel in ethanol (a) and its recovery (b).

responsive tests, it can be deduced from the time axis of the figures that the temperature-response rate was the fastest. Additionally, the center angle and curvature presented the same trend because of the special stimuli response mechanisms of PDMAEMA and PNIPAM. This situation may be different in bilayer hydrogels prepared from different monomers.

### 3.3 4-Arm gripper

Both ends of the bilayer hydrogel are regarded as particles whose motion can be de-composited into the horizontal and vertical directions. The midpoint of the hydrogel was set as the origin of the reference system, as Fig. 8a shows. When the hydrogel bent in response to stimuli, the moving track included the process of clamping; thus, a 4-arm gripper was manufactured. As concluded from the former chapter, the thermal response rate was the fastest, so the gripper was driven by temperature. Fig. 8b shows the gripping and release process of the 4-arm gripper. As Fig. 8c shows, for a faster and more convenient grip, the 4-arm gripper was first immersed in hot water (40 °C) and then subsequently adjoined close above the copper sheet. It took 20 s to generate an equal force for lifting an object against gravity. When the “arms” bent inwards and caught the object, the gripper was pulled up out of a high-temperature environment and then moved to a low-temperature environment (25 °C). Due to the thermal property of the bilayer hydrogel, the “arms” bent outwards, releasing the object within 142 s.

### 3.4 Conductivity of bilayer hydrogels and thermistor

The D layer was conductive for containing ionic polymers (PDMAEMA and PSS). The average resistance was around 44.8 kΩ. While in the N layer, conventional polymers are non-conductive; therefore, CB was added in the N layer to improve its electrical conductivity. The graphite phase in carbon black

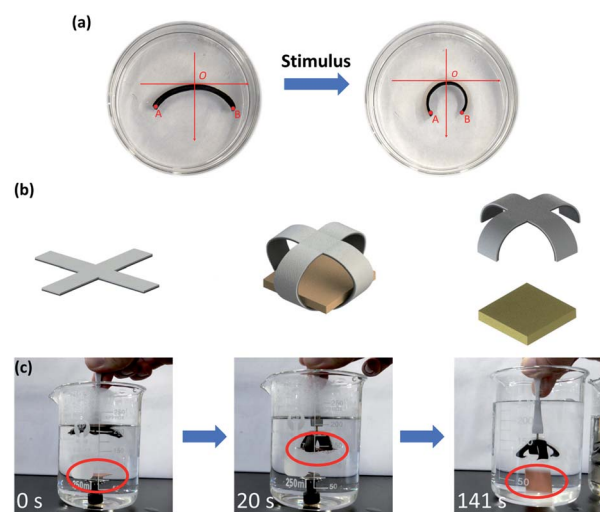


Fig. 8 (a) Bending behavior of the bilayer hydrogel and reference system; schematic illustration (b) and digital images (c) of the gripping and release using the 4-arm gripper (the copper sheet is marked by the red circle).



Table 1 Voltage division (V) between the LED and bilayer hydrogel

| Working condition   | Hydrogel | LED  | Rated voltage |
|---------------------|----------|------|---------------|
| 25 °C (no hydrogel) | ×        | 4.99 | 5.00          |
| 25 °C               | 2.98     | 1.99 | 5.00          |
| 50 °C               | 1.91     | 3.02 | 5.00          |
| 25 °C               | 3.05     | 1.93 | 5.00          |

contains conjugated  $\pi$ -bonds that allow electrons to move freely. In addition, CB was well-dispersed, and *in situ* polymerization maintained the original locations of CB, forming a continuous conductive network; thus, the bilayer hydrogel was conductive. The bilayer hydrogel was added into a circuit as a thermistor to further prove its conductivity and thermal-responsive properties. This circuit included a regulated power supply (5 V), an LED, the bilayer hydrogel, and some copper wires, as shown in Fig. S5.† When the hydrogel was not connected to the circuit, the voltage of the LED tested by the multi-meter was very close to the total voltage due to line loss. Once the hydrogel was connected to the circuit, the voltage of the LED was divided, as Table 1 shows. Initially, the hydrogel was immersed in cold water (25 °C) with a divided voltage of nearly 1.91 V. Subsequently, the hydrogel was quickly immersed in hot water (50 °C) and then placed in cold water (25 °C), which changed the voltage to 1.91 V and then back to 3.05 V, demonstrating the thermal-responsive properties of the hydrogel. Apart from the value change in the multi-meter, the brightness of the LED was also used as an observation index, as Fig. 9b shows. The brightness of the LED changed in the order of dark–bright–dark (Fig. 9a) after immersing the hydrogel in

water at different temperatures with the order: cold (25 °C) – hot (50 °C) – cold (25 °C).

During polymerization in the N layer, CB was well dispersed, and each position was fixed after gelling. As mentioned in the former section, a high environmental temperature caused the positive bending of the bilayer hydrogel and the shrinkage of the N hydrogel. The deformation reduced the distance between CB, increasing its density. In this way, the increase in the conductive material per unit volume reduced the resistance of the bilayer hydrogel; thus, the resistance of the hydrogel decreased when the temperature increased and *vice versa*, which explains the value changes in Table 1. From a macroscopic view, the deformation caused by a force directly acting on the hydrogel also changed its resistance. Because axial compression is difficult to achieve, axial stretching was used. It is shown in Fig. 9c and d that the resistance of the hydrogel increased with the degree of stretching and *vice versa*. It can be concluded that the bilayer hydrogel is conductive, which was affected by volume changes, whether caused by a stimuli response or an external force.

### 3.5 Finger movement monitor

A finger movement monitor was developed based on the conclusions drawn in the former chapter, in which the resistance of the bilayer hydrogel was correlated with stretching deformation. The assembled monitor is shown in Fig. 10a. The resistance changing along with finger movement was divided into different phases (bending 0°, 45°, and 90°). Initially, the finger was straightened, and the change in resistance was zero. As the bending degree of the finger increased and decreased, the resistance of the bilayer hydrogel changed correspondingly, and each phase was maintained for a short time, as Fig. 10b illustrates. In each phase, the resistance varied enough for it to be distinguished; therefore, according to the resistance data, when the finger completed at least one movement cycle, it is

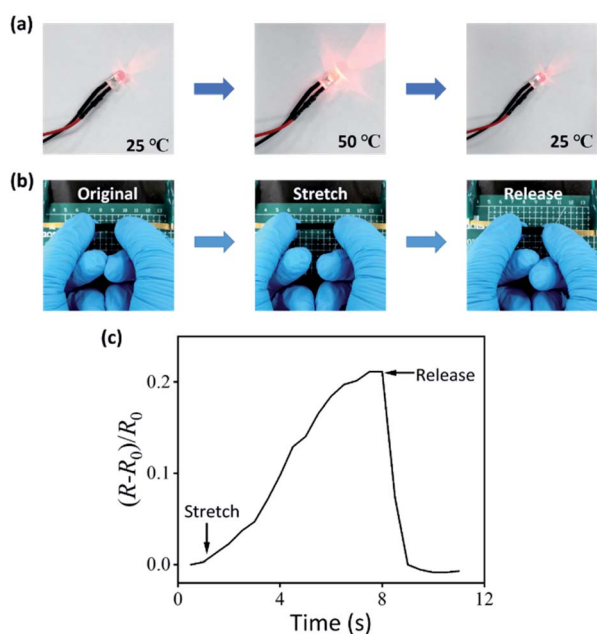


Fig. 9 (a) Brightness changes of the LED when the bilayer hydrogel was immersed in deionized water in the order of 25 °C–50 °C–25 °C. The correlation between (b) stretching degree and (c) resistance change rate of the bilayer hydrogel.

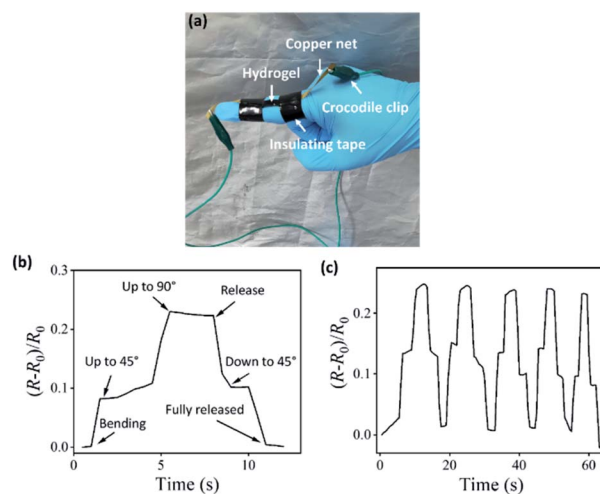


Fig. 10 (a) Image of the assembled finger movement monitor; (b) the correlation between bending states of finger and resistance change rate of the bilayer hydrogel; (c) repeated finger movement monitoring (5 times).





easy to judge which phase the finger is in. Furthermore, a repeatability test was carried out, as shown in Fig. 10c. Each phase of finger movement can be clearly distinguished, which ensures that the hydrogel can be used as a reliable monitor.

## 4. Conclusions

PDMAEMA/PNIPAM bilayer hydrogel and the single-layer hydrogels corresponding to each layer were designed and prepared. The stimuli-responsive properties and deformation mechanisms of the bilayer hydrogel were studied *via* the swelling/de-swelling state of the single-layer hydrogels and bending of the bilayer hydrogel. The results indicated that the bilayer hydrogel was responsive to temperature, pH, salt, and ethanol and reverted without intense or prolonged simulation. Additionally, the stimulus that generated the fastest response was temperature, and the SDS concentration and temperature were also explored. A high concentration of SDS slowed the response speed, while a high temperature accelerated it. The bilayer hydrogel was rendered conductive by adding uniformly dispersed CB. When the hydrogel was deformed, the density of the conductive material per unit volume increased or decreased, which affected the resistance of the hydrogel. Due to the stimuli-responsive and conductive properties, we developed a 4-arm gripper, thermistor, and finger movement monitor using the hydrogel, which could grip and release, change their resistance with temperature, and monitor finger motions, respectively. These multi-stimuli-responsive bilayer hydrogels presented great potential in soft robots, multi-stimuli-dependent resistors and human body monitors.

## Conflicts of interest

There are no conflicts to declare.

## Acknowledgements

This work is supported by the Excellent Youth Foundation of Anhui Scientific Committee (Grant No. 1808085J30), the National Natural Science Foundation of China (Grant No. 11872001 and 12172002), the Key Research and Development Program Projects in Anhui Province (Grant No. 202004h07020026) and Anhui Province Innovation Foundation for Returnees.

## Notes and references

- J. P. Gong, *Soft Matter*, 2006, **2**(7), 544–552.
- W. Yang, H. T. Wang, T. F. Li and S. X. Qu, *Sci. China, Ser. G: Phys., Mech. Astron.*, 2018, **62**(1), 14601.
- E. M. Ahmed, *J. Adv. Res.*, 2015, **6**(2), 105–121.
- Z. Ayar, M. Shafieian, N. Mahmoodi, O. Sabzevari and Z. Hassannejad, *J. Appl. Polym. Sci.*, 2021, **138**(40), 51167.
- H. Ding, B. Li, Z. Liu, G. Liu, S. Pu, Y. Feng, D. Jia and Y. Zhou, *Adv. Healthcare Mater.*, 2020, **9**(14), 2000454.
- M. Wu, Y. Zhang, Q. Liu, H. Huang, X. Wang, Z. Shi, Y. Li, S. Liu, L. Xue and Y. Lei, *Biosens. Bioelectron.*, 2019, **142**, 111547.
- Y. H. Yan, L. H. Rong, J. Ge, B. D. B. Tiu, P. F. Cao and R. C. Advincula, *Macromol. Mater. Eng.*, 2019, **304**(7), 1800720.
- X. Zhang, J. Liu, Y. Gao, J. Hao, J. Hu and Y. Ju, *Soft Matter*, 2019, **15**(23), 4662–4668.
- B. Sharma, A. Singh, T. K. Sarma, N. Sardana and A. Pal, *New J. Chem.*, 2018, **42**(8), 6427–6432.
- J. F. Chen, Q. Lin, H. Yao, Y. M. Zhang and T. B. Wei, *Mater. Chem. Front.*, 2018, **2**(5), 999–1003.
- Y. Q. Liu, K. G. Xu, Q. Chang, M. A. Darabi, B. J. Lin, W. Zhong and M. Xing, *Adv. Mater.*, 2016, **28**(35), 7758–7767.
- T. Aida, Z. Sun, Y. Yamauchi, F. Araoka, Y. S. Kim, J. Bergueiro, Y. Ishida, Y. Ebina, T. Sasaki and T. J. A. C. Hikima, *Angew. Chem., Int. Ed.*, 2018, **57**(48), 15772–15776.
- Z. Zhu, E. Senses, P. Akcora and S. A. Sukhishvili, *ACS Nano*, 2012, **6**(4), 3152–3162.
- T. Inadomi, S. Ikeda, Y. Okumura, H. Kikuchi and N. Miyamoto, *Macromol. Rapid Commun.*, 2014, **35**(20), 1741–1746.
- P. Sun, H. Zhang, D. Xu, Z. Wang, W. Liufang, G. Guorong, G. Hossain, J. Wu, R. Wang and J. Fu, *J. Mater. Chem. B*, 2019, **7**(16), 2619–2625.
- Q. Zhao, Y. Liang, L. Ren, Z. Yu, Z. Zhang, F. Qiu and L. Ren, *J. Mater. Chem. B*, 2018, **6**(8), 1260–1271.
- Q. Shi, H. Xia, P. Li, Y.-S. Wang, L. Wang, S.-X. Li, G. Wang, C. Lv, L.-G. Niu and H.-B. Sun, *Adv. Opt. Mater.*, 2017, **5**(22), 1700442.
- Z. L. Wu, M. Moshe, J. Greener, H. Therien-Aubin, Z. Nie, E. Sharon and E. Kumacheva, *Nat. Commun.*, 2013, **4**, 1586.
- A. S. Gladman, E. A. Matsumoto, R. G. Nuzzo, L. Mahadevan and J. A. Lewis, *Nat. Mater.*, 2016, **15**(4), 413–418.
- R. Yang and Y. Zhao, *Angew. Chem., Int. Ed.*, 2017, **56**(45), 14202–14206.
- H. W. Huang, M. S. Sakar, A. J. Petruska, S. Pane and B. J. Nelson, *Nat. Commun.*, 2016, **7**, 12263.
- X. Zhang, C. L. Pint, M. H. Lee, B. E. Schubert, A. Jamshidi, K. Takei, H. Ko, A. Gillies, R. Bardhan, J. J. Urban, M. Wu, R. Fearing and A. Javey, *Nano Lett.*, 2011, **11**(8), 3239–3244.
- J. Zheng, P. Xiao, X. Le, W. Lu, P. Théato, C. Ma, B. Du, J. Zhang, Y. Huang and T. Chen, *J. Mater. Chem. C*, 2018, **6**(6), 1320–1327.
- S. Xiao, Y. Yang, M. Zhong, H. Chen, Y. Zhang, J. Yang and J. Zheng, *ACS Appl. Mater. Interfaces*, 2017, **9**(24), 20843–20851.
- Q. Wang, Z. Liu, C. Tang, H. Sun, L. Zhu, Z. Liu, K. Li, J. Yang, G. Qin, G. Sun and Q. Chen, *ACS Appl. Mater. Interfaces*, 2021, **13**, 10457–10466.
- W. Huo, H. An, S. Chang, S. Yang, Y. Huang, X. Zhang, X. Hu and H. Zhang, *Polymers*, 2021, **13**(11), 1753.
- Z. Zhang, Z. Chen, Y. Wang, J. Chi, Y. Wang and Y. Zhao, *Small Methods*, 2019, **3**(12), 1900519.
- A. Navaei, H. Saini, W. Christenson, R. T. Sullivan, R. Ros and M. Nikkhah, *Acta Biomater.*, 2016, **41**, 133–146.



## Paper

- 29 S. Xia, S. Song, F. Jia and G. Gao, *J. Mater. Chem. B*, 2019, **7**(30), 4638–4648.
- 30 J. Chen, Q. Peng, T. Thundat and H. Zeng, *Chem. Mater.*, 2019, **31**(12), 4553–4563.
- 31 B. B. Ying, Q. Y. Wu, J. Y. Li and X. Y. Liu, *Mater. Horiz.*, 2020, **7**(2), 477–488.
- 32 L. Han, Y. Zhang, X. Lu, K. Wang, Z. Wang and H. Zhang, *ACS Appl. Mater. Interfaces*, 2016, **8**(42), 29088–29100.
- 33 T. Zhan, H. Xie, J. Mao, S. Wang, Y. Hu and Z. Guo, *ChemistrySelect*, 2021, **6**(17), 4229–4237.
- 34 P. Jiang, S. W. Chen, L. D. Lv, H. M. Ji, G. Li, Z. C. Jiang and Y. Q. Wu, *J. Nanosci. Nanotechnol.*, 2020, **20**(3), 1799–1806.
- 35 H. Sun, J. Chen, X. Han and H. L. Liu, *Mater. Sci. Eng., C*, 2018, **82**, 284–290.
- 36 Y. Cheng, K. Ren, D. Yang and J. Wei, *Sens. Actuators, B*, 2018, **255**, 3117–3126.
- 37 N. Uehara and M. Ogawa, *Langmuir*, 2014, **30**(22), 6367–6372.
- 38 M. Meewes, J. Ricka, M. De Silva, R. Nyffenegger and T. Binkert, *Macromolecules*, 1991, **24**(21), 5811–5816.
- 39 S. B. Lee, S. C. Song, J. I. Jin and Y. S. Sohn, *Macromolecules*, 1999, **32**(23), 7820–7827.

